PROBING PHOTOSYNTHESIS ON A PICOSECOND TIME SCALE

EVIDENCE FOR PHOTOSYSTEM I AND PHOTOSYSTEM II FLUORESCENCE IN CHLOROPLASTS

MICHAEL SEIBERT *and* ROBERT R. ALFANO

From GTE Laboratories Inc., Waltham, Massachusetts 02154, and the Physics Department, City College of New York, New York 10031

ABSTRACT Fluorescent emission kinetics of isolated spinach chloroplasts have been observed at room temperature with an instrument resolution time of 10 ps using a frequency doubled, mode-locked Nd:glass laser and an optical Kerr gate. At 685 nm two maxima are apparent in the time dependency of the fluorescence; the first occurs at 15 ps and the second at 90 ps after the flash. The intervening minimum occurs at about 50 ps. On the basis of theoretical models, lifetimes of the components associated with the two peaks and spectra (in escarole chloroplasts), the fluorescence associated with the first peak is interpreted as originating from Photosystem I (PSI) (risetime $\leq$10 ps, lifetime $\leq$10 ps) and the second peak from Photosystem II (PSII) (lifetime, 210 ps in spinach chloroplasts and 320 ps in escarole chloroplasts). The fact that there are two fluorescing components with a quantum yield ratio $\leq$0.048 explains the previous discrepancy between the quantum yield of fluorescence measured in chloroplasts directly and that calculated from the lifetime of PSII. The 90 ps delay in the peak of PSII fluorescence is probably explained by energy transfer between accessory pigments such as carotenoids and Chl a. Energy spillover between PSI and PSII is not apparent during the time of observation. The results of this work support the view that the transfer of excitation energy to the trap complex in both photosystems occurs by means of a molecular excitation mechanism of intermediate coupling strength. Although triplet states are not of major importance in energy transfer to PSII traps, the possibility that they are involved in PSI photochemistry has not been eliminated.

INTRODUCTION

In higher plant photosynthesis, energy is first transferred from the absorbing accessory pigments to the reaction center complexes of Photosystem I (PSI) and Photosystem II (PSII). The stage is then set for the initiation of the oxidation-reduction reactions which drive the splitting of water, phosphorylation, and carbon reduction (1). To understand the primary energy transfer reactions which take place

within a nanosecond, it is of fundamental importance to study the processes in this time domain. Elucidation of the exact mechanism will involve knowledge of the kinetics of fluorescent emission as well as those of singlet to triplet crossing, nonradiative decay and, of course, trapping (the pathway which leads to photochemistry).

Using both direct flash (hydrogen flash lamps) and phase methods, several groups (2–9) have estimated the mean fluorescent lifetime of in vivo chlorophyll (Chl) and have shown it to be dependent on the intensity of the exciting flash (3, 10) and on photosynthetic activity (11, 12). Recently, Merkelo et al. (13), using nanosecond light pulses emitted from a mode-locked He-Ne laser (14), reported a decay time of 1.5 ns for *Chlorella pyrenoidosa* fluorescence corresponding to a value Müller et al. (10) found at high actinic intensity. Mar et al. (15) reported similar lifetimes for DCMU poisoned algae using the same technique. In all of these studies only a single fluorescing species was observed.

With the advent of picosecond light pulses emitted by mode-locked ruby and Nd:glass lasers, the direct observation of the time development of the initial stages of the photosynthetic process on a picosecond time scale became possible. An ultrafast optical Kerr gate or shutter (16) operated by a mode-locked Nd:glass laser has in fact permitted the measurement of vibrational relaxation times and fluorescent lifetimes in organic dye molecules (17, 18) with an instrument time resolution in the order of 10 ps. This communication is a continuation of previous preliminary work (19, 20) using an optical Kerr gate in the study of photosynthesis and reports on kinetics, lifetimes, and spectra of spinach and escarole chloroplast chlorophyll on a picosecond time scale.

MATERIALS AND METHODS

Laser-Optical Kerr Gate Apparatus

A schematic diagram of the experimental apparatus is shown in Fig. 1. The laser consists of a Brewster cut 7½ in × ½ in Owens-Illinois glass rod (ED-2, Owens-Illinois, Toledo, Ohio), a Korad (K-1) laser head (Korad Div., Union Carbide Corp., Santa Monica, Calif.), a 10 meter radius of curvature, 100% reflectivity rear dielectric mirror, a 50% reflectivity dielectric wedge output mirror (~30 min), and a Kodak Q-switch dye cell (type 9860 Kodak dye). Light output at 1.06 μm (~5×10^9 W)[1] passes through a 2 cm potassium-dihydrogen-phosphate (KDP) second-harmonic generator crystal with as much as 10% conversion to the harmonic at 0.53 μm. A typical laser flash consists of about 50 pulses separated from each other by the cavity round-trip time of 5.5 ns. Pulse widths of 6 ps at 1.06 μm and 4 ps at 0.53 μm were measured by the two-photon fluorescence technique (21).

A dielectric mirror (M_1) which transmits 70% at 1.06 μm and reflects 90% at 0.53 μm directs the different wavelength pulses along separate delay paths. The chloroplast sample is excited by the 0.53 μm beam (0.5 cm in diameter at the sample surface) which has been circularly polarized with a quarter wave plate. Fluorescence from the chloroplasts is collected and collimated through the optical gate (16, 17), a system of two crossed Polaroids with a 1 cm

[1] Averaged over the length of the pulse train (~200 ns).

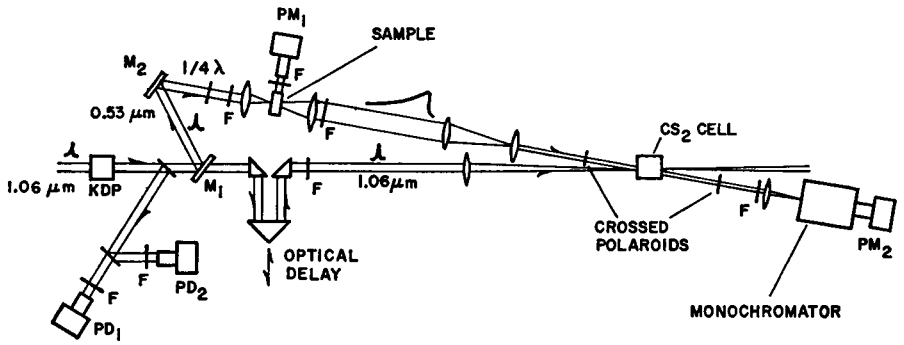

FIGURE 1 A schematic diagram of the laser-optical Kerr gate apparatus. PD, photodiode; M, mirror; F, optical filter; ¼λ, quarter wave plate; and PM, photomultiplier tube.

path length cell of carbon disulfide placed in between. The 1.06 μm beam follows a path which can be adjusted by a variable optical delay and is reduced to 1 mm in diameter upon passage through the carbon disulfide cell. Its function is to induce a short-lived birefringence in the CS_2 thus allowing light along the 0.53 μm path to pass through the crossed polaroid configuration only during the induced birefringence. The zero point of the optical gate is determined by the coincidence in time and space of the 1.06 μm and 0.53 μm pulses with buffer solution substituted for the chloroplast sample in the cuvette. This "prompt" curve is 8 ps wide at half-maximum with a peak to noise level of 100 to 1 over the experimental time range. By adjusting the optical delay (moving the prism) of the 1.06 μm beam, the fluorescent output can be sampled at various times with respect to the actinic pulse.

After passing through the gate the fluorescence is focused onto the entrance slits of a spectrometer(¼ m Jarrel-Ash monochromator [Jarrel-Ash Co., Waltham; Mass.] combined with an RCA 7265 photomultiplier tube) so that the time dependence of the fluorescence can be recorded as a function of the wavelength. It is clear that the extremely rapid response (~10 ps) of this instrument is not due to the photomultiplier or its associated electronics (which in fact is relatively slow so that the data is integrated over the time of the output train of pulses) but to the extremely short sampling period allowed by the optical Kerr gate light shutter. To correct the data for differences in laser output from shot to shot, the intensity of the 1.06 μm and 0.53 μm beams (ITT S-20 photodiodes) and the total fluorescent intensity (ITT S-20 photodiode or RCA S-1 photomultiplier tube) were also detected and displayed simultaneously with the corresponding gated fluorescence (at the particular delay time and wavelength) on a dual beam oscilloscope (Tektronics 556; Tektronics, Inc., Beaverton, Ore.) using appropriate delay cables.

The multiple pulse method is suitable for measuring fluorescent lifetimes as long as (*a*) the fluorescent component being observed recovers within the time between pulses (the case in the present work) and (*b*) there are no long term effects which *significantly* alter the lifetime of that component. This second point was investigated since any Chl which is oxidized does not return to the original state within the period of the pulse train and since the lifetime of Chl fluorescence (PSII) increases with the level of the actinic light (10). The data in Fig. 2, a plot of the total fluorescence versus the total energy density of the 0.53 μm beam (the integrated energy of the entire train), describe a straight line passing through the origin. If the population of reaction center complexes were oxidized to a significant extent, the extrapolation of the curve would pass to the right of the origin (Fig. 4 of ref. 22). From the average energy

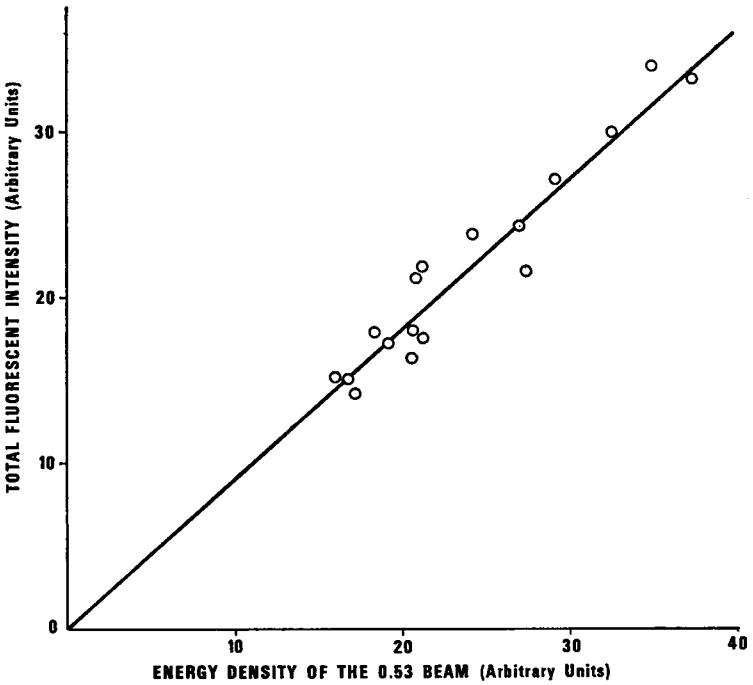

FIGURE 2 The total fluorescent intensity (signal recorded by PM_1, in Fig. 1) plotted as a function of the energy density of the 0.53 μm flash.

density per pulse incident on the sample (~600 ergs/cm^2) one can estimate[2] that the experiments were performed at a Chl oxidation level corresponding to less than 5% of the saturation value. In addition, the fluorescent lifetimes which we observe correspond to the low intensity limits (10). Therefore, use of the entire train is fully justified under our experimental conditions.

Chloroplasts

Spinach (*Spinacia oleracea*) and escarole (*Cichorium endivia*) chloroplasts were prepared daily by a slight modification of the methods of Avron (24) and Cramer and Butler (25). 50 g of de-veined, washed leaves were homogenized in 150 ml of ice-cold buffer solution (0.4 M sucrose, 0.05 M Tris-HCl, 0.01 M NaCl, and 0.01 M ascorbic acid, pH 7.6) for 20 s at a low speed using a Waring Blender. The resultant slurry was filtered through a double layer of cheesecloth and centrifuged for 1.5 min at 500 *g*. The supernate was then centrifuged for 7 min at 1,000 *g* and the pellet washed once in buffer solution (10 min at 2,000 *g*). For experimental purposes the preparations were diluted in the buffer as desired and continuously

[2] This was done by observing the complete saturation curve for laser-induced reaction center bacteriochlorophyll (BChl) oxidation in bacterial chromatophores (23) and comparing the absorbance of the chloroplast samples at 0.53 μm (the activation wavelength used in the present study) with that of the bacterial samples at 0.69 μm (the actinic wavelength of the ruby laser used to obtain the bacterial saturation curves). It was assumed that in vivo Chl and BChl saturate at approximately the same quantum level of absorbed photons and that chloroplasts and chromatophores have about the same size photosynthetic unit.

circulated to and from an ice-cold, black cloth covered reservoir by means of a vibrostaltic pump (The Chemical Rubber Company, Cleveland, Ohio). The reservoir to cuvette volume ratio was 15 to 1 and the time between flashes was 3–5 min. Thus the chloroplasts were always essentially dark adapted at the beginning of the flash. A dry stream of nitrogen directed at the cuvette prevented condensation on the optical surfaces. Chl concentrations were obtained using the method of Arnon (26) and all work was done in the dark.

RESULTS

Kinetics

In Fig. 3 the relative fluorescence of spinach chloroplasts at 685 nm is plotted as a function of the delay time with respect to the 0.53 μm actinic flash. The following

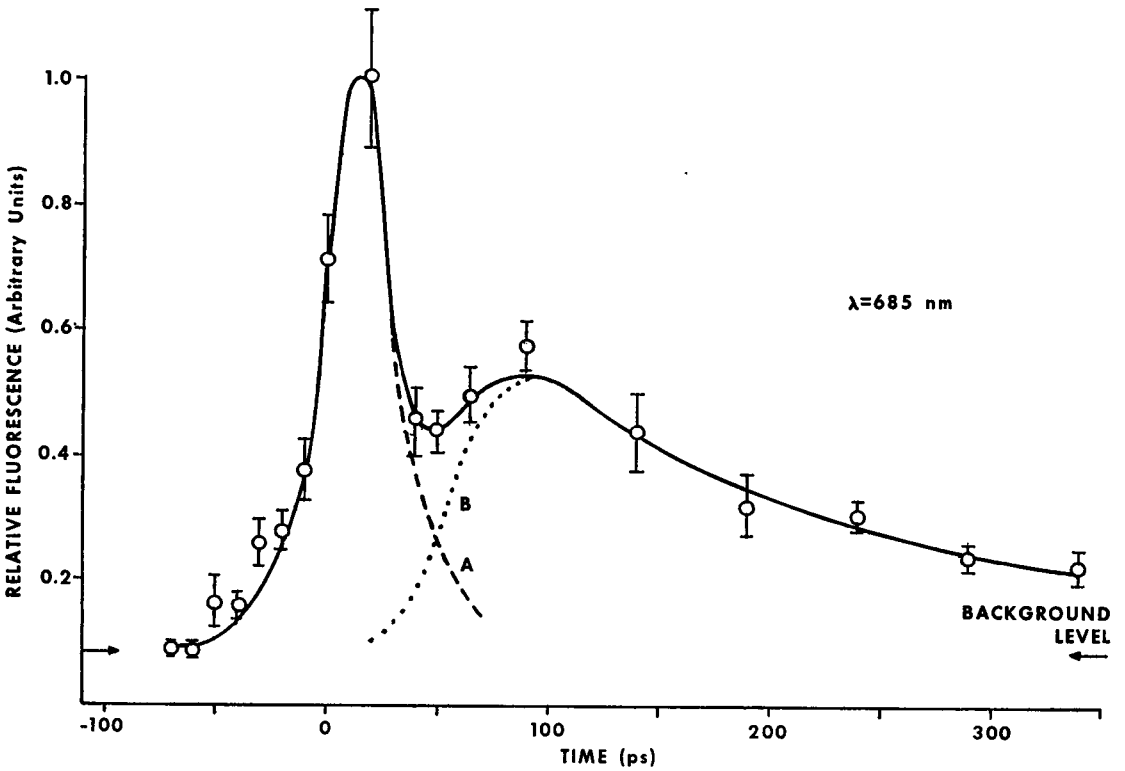

FIGURE 3 The time dependence of fluorescent emission from spinach chloroplasts at 685 nm after excitation by a 4 ps pulse of 0.53 μm light. The fluorescent emission at a particular time delay was obtained by normalizing the PM_2 signal (Fig. 1) for the amount of total fluorescence (PM_1 signal in Fig. 1) and the intensity of the 1.06 μm flash (16). This normalization was necessary because the intensity of the flash was not reproducible. Each open circle represents a mean number of 6.5 (range was 4–14) individual laser flashes. The dashed curve, *A*, is an extrapolation of the decay of the first peak while the dotted curve, *B*, is merely the difference between the solid curve and curve *A*. The error bars represent 1 standard error of the arithmetic mean. Monochromator bandwidth, 6.6 nm; total Chl concentration, 35 μg/ml.

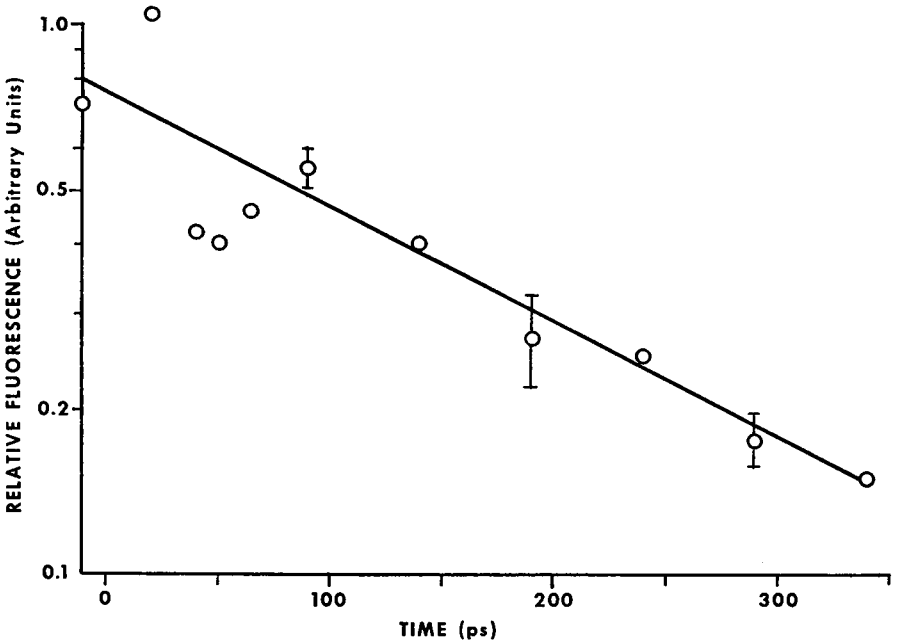

FIGURE 4 The logarithm of the difference between the fluorescent intensity and the background level in Fig. 3 plotted at various times. The best straight line through the data after 90 ps gives a lifetime of 210 ps for the decay of the second peak. Note that the data point at 90 ps lies above the line, a fact considered when the solid curve in Fig. 3 was drawn.

salient features immediately noted are: (*a*) the risetime of fluorescence is ≤ 10 ps, (*b*) peaks are apparent at approximately 15 ps and 90 ps after excitation, (*c*) a trough is evident at 50 ps, and (*d*) the kinetics subsequent to the second peak appear to decay exponentially. Picosecond fluorescent emission kinetics previously reported for escarole chloroplasts (19, 20) have shown this same double peak phenomenon (maxima at 0 and 90 ps). The apparent risetime of the second peak is in the order of 50 ps. Decay kinetics are graphed in Fig. 4, which is a first order plot (logarithm of the difference between the fluorescent intensity and the background level as a function of time) of the data depicted in Fig. 3. From the slope of this curve one obtains a lifetime of 210 $\pm$ 25 ps for the second kinetic peak. A similar treatment resulted in a lifetime of 320 ps for the second peak of escarole chloroplasts (19, 20). It should be emphasized that the second kinetic peak has to be a result of energy input at time zero since no spurious laser pulse occurs within the first 100 ps. Further verification of this fact is resultant from the observation that organic dyes (18) under the same experimental conditions decay from a single peak.

Emission Spectrum

The fluorescent emission spectrum for escarole chloroplasts at time zero (the initial peak seemed to be closer to the zero point for escarole chloroplasts than for spinach

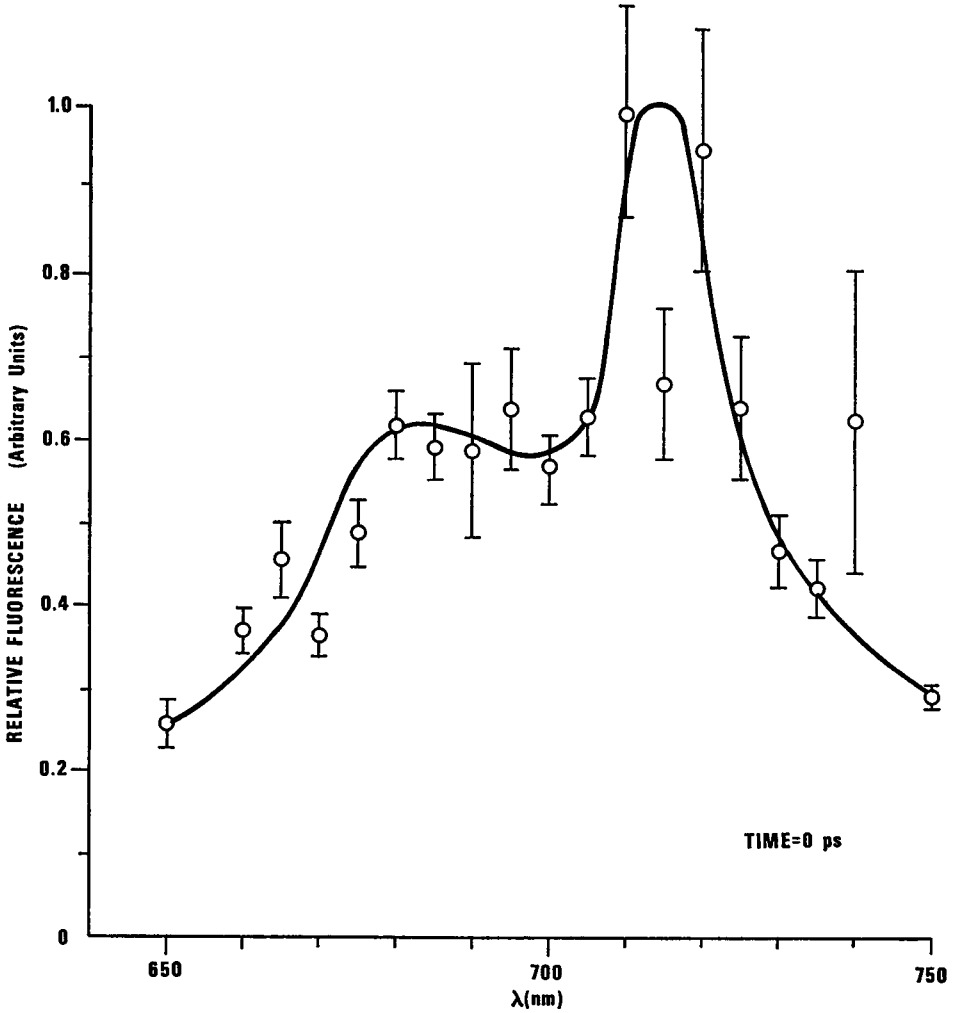

FIGURE 5 A fluorescent emission spectrum for escarole chloroplasts taken at time equals zero under conditions similar to those in Fig. 3. The data represents the normalized results of two separate experiments and each open circle represents a mean number of 9.5 (the range was 4–16) individual flashes. Besides the corrections mentioned in the legend of Fig. 3, these data were also adjusted for the spectral sensitivity of the monochromator and detector. The error bars represent 1 standard error of the arithmetic mean. Bandwidth, 6.6 nm.

chloroplasts but this may be within experimental error) is plotted in Fig. 5. It represents the normalized results of two experiments performed on different days. Peaks at 683 nm and 714 nm are quite apparent. Although the spectrum has been corrected for sensitivity of the photomultiplier tube and the monochromator over the wavelength region, the relative peak heights must not be emphasized due to self-absorption of the rather dense chloroplast sample required to observe a signal on this time scale. The point at 715 nm misses the curve by a substantial amount (probability

$\simeq$0.27%), but limited data from only one experiment was available at this particular wavelength. An accurate spectrum for the second kinetic peak (90 ps after the flash) is not as yet available, but a preliminary experiment is suggestive of a broad fluorescence band with a narrow peak superimposed at around 690 nm. Consistent with this result was a densitometer scan of a photographic negative exposed to escarole chloroplast fluorescence passing through a ½ m Jarrel-Ash monochromator with the optical gate removed. The trace represents picosecond laser-flash activated fluorescence integrated over all time and shows peaks at 686 nm and 713 nm with a shoulder at 694 nm.

DISCUSSION

For nearly 20 yr now various groups have been measuring in vivo Chl lifetimes with the rather tacit assumption that there was only one observable fluorescing component. In fact, if a sample has two fluorescing components, depending on the relative amplitudes and quantum yields, the lifetime of that fluorescing sample may bear little resemblance to the lifetime of either of its components, as measured by the phase technique (27). If the lifetime of one of the two components is very short compared with the flash duration in pulse experiments, only one would be easily observable.

Evidence for Identification of Fluorescence from Both Photosystems

With the advantage of an instrument resolution time of about 10 ps, we have been able to observe two peaks in the fluorescent emission kinetics of spinach chloroplasts (Fig. 3). To test how two or more species might have to be related in order to give the observed two peaks, the following five models were considered: (*a*) one absorbing species which transfers energy to a second fluorescing species; (*b*) one absorbing species which both fluoresces and transfers energy to a second fluorescing species; (*c*) two dependent absorbing species only one of which fluoresces; (*d*) two independent species which both absorb and fluoresce; and (*e*) two independent absorbing species, one of which fluoresces and the other which transfers energy to a third fluorescing species. Fig. 6 shows energy level diagrams for the models and pictorially summarizes the time dependence of fluorescent emission predicted by solving the rate equations in the respective cases. For those who are interested, the rate equations and their solutions are given in the Appendix. Only those models which postulate at least two independently (on this time scale) absorbing and fluorescing species display two peaks in the calculated time dependence of fluorescence. One immediately suspects the possibility that fluorescent emission from both PSI and PSII have been observed in chloroplasts.

Borisov and Il'ina (27) based on indirect methods have placed an upper limit of 30 ps on the fluorescent lifetime of PSI Chl in pea chloroplasts and digitonin fractions. The upper limit for the lifetime of the first peak in Fig. 3 is 10 ps, well within

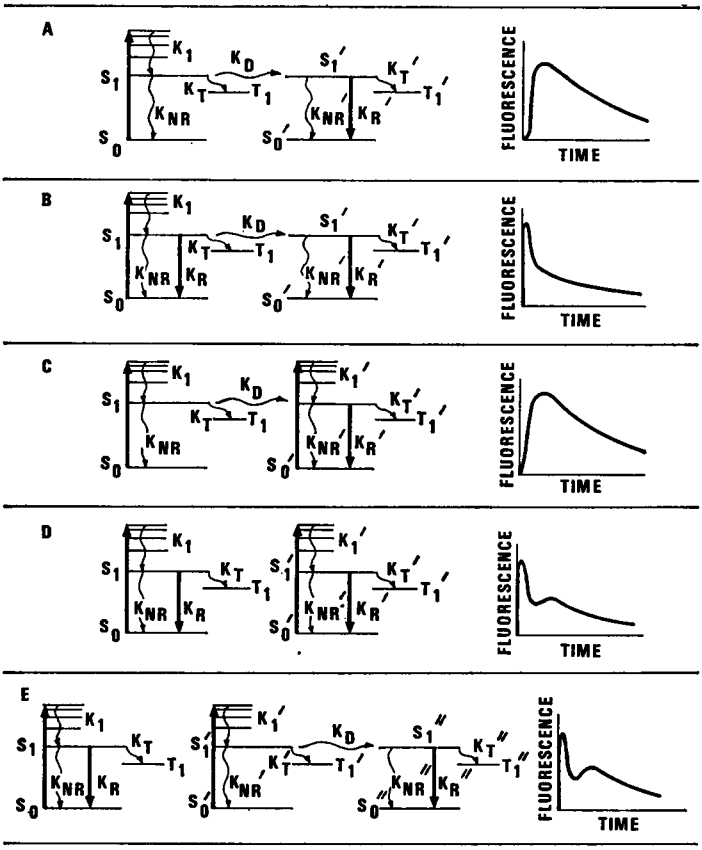

FIGURE 6 Energy level diagrams and predicted fluorescent emission curves for Models A–E as described in the text. The equations governing the time dependence of fluorescent emission are given in the Appendix. The first order rate constants are defined as follows: K_1 is the vibrational decay constant for the excited electronic singlet state, S_1; K_R is the radiative decay constant between S_1 and the ground electronic singlet state, S_0; K_{NR} is the nonradiative decay constant between S_1 and S_0; K_T is the rate constant for crossing from S_1 to the triplet state, T_1; and K_D is the rate constant for energy transfer between two excited singlet states of different species. The unprimed, primed, and double primed labels denote different species.

the predicted value for PSI. It should be emphasized that spinach Chl not associated with photochemical activity has a quantum yield of 0.027 (28), a value much too high to qualify such Chl as the source of fluorescence in the case of the first peak. The lifetime of PSII has been estimated many times for different species and is in the order of several hundreds of picoseconds (350 ps for *Chlorella* cells and 380 ps for sugarbeet leaves [10]; 320 ps for escarole chloroplasts [19]) at low actinic intensity. The second peak in Fig. 3 decays with a lifetime of 210 ps which is consistent with, though lower than the 700 ± 200 ps (9) previously reported for the lifetime of fluorescence in spinach chloroplasts (predominantly PSII). Since the

lifetime reported in ref. 9 for *Chlorella pyrenoidosa* is about twice that reported in ref. 10, it is likely that the 700 ps result reported for spinach chloroplasts is also high.

The spectrum in Fig. 5 (the first kinetic peak of escarole chloroplasts, see the figure in ref. 19 which is similar to Fig. 3 in the present work), although it appears to differ from that of the second kinetic peak, is not typical of normal room temperature PSI fluorescence (28–30). Since this spectrum was obtained using a higher Chl concentration than is normal for fluorescent studies, we interpret Fig. 5 as PSI fluorescence distorted by self-absorption of the short wavelength component. Fig. 4 in ref. 30 clearly shows this concentration effect in PSI enriched particles at 77°K. In addition, the ratio of long wavelength (720 nm) to short wavelength (683 nm) fluorescence is about three times greater in PSI enriched fractions than in PSII enriched particles (28–30) at room temperature.

On the basis of the models, lifetimes and spectra, then, we conclude that the first peak in Fig. 3 is due to fluorescence from PSI and the second from PSII.

Resolution of the Quantum Yield Discrepancy

When Brody and Rabinowitch (2) measured the fluorescent lifetime of Chl in *Chlorella*, they found that there was a large discrepancy between the fluorescent yield (ϕ) which they calculated using the equation $\phi = \tau/\tau_0$ (where τ_0 is the natural lifetime) and the fluorescent yield which Latimer et al. (31) measured directly. While much of the discrepancy could be explained by differences in the light levels used to obtain the two experimental results and the inefficient transfer of energy from carotenoids to Chl (32), there was still a difference between the yields obtained by the two methods even after corrections were made (32). The results of the present work show that there are two fluorescing components in spinach chloroplasts with substantially different lifetimes. Since the amount of short lifetime component (PSI) was not taken into account in previous quantum yield calculations, these estimates have always been higher than the directly measured values. PSI, then, is the "nonfluorescing," absorbing species which has been postulated to explain the discrepancy (2, 29, 32).

Table I gives a summary of the kinetic data as well as a comparison of the calculated and measured quantum yields for PSI and PSII fluorescence in spinach. The yield calculated for PSII in chloroplasts is very close to that measured in PSII enriched particles (28). That calculated for PSI in chloroplasts is lower than the value measured in PSI fractions (28). Presumably Chl not connected to photochemical activity but still associated with the PSI enriched fraction (28) greatly increases the apparent quantum yield of PSI.

Delay in Fluorescence

In Fig. 7, Models D and E are fitted to the data of Fig. 3. The deviation of the calculated curves from the experimental curve near $t = 0$ is due to the use of a delta

TABLE I

KINETIC AND QUANTUM YIELD PARAMETERS FOR SPINACH FLUORESCENCE

	PSI	PSII	PSI/PSII	Chloro-plasts	Ref.
Risetime (ps)*	≤ 10	90‡	—	—	Fig. 3
Lifetime (ps)*	≤ 10	210 ± 25	—	—	Figs. 3, 4
Calculated quantum yield§	≤ 0.00066	0.0138 ± 0.0018	≤ 0.048	—	Figs. 3, 4
Measured quantum yield‖	0.003	0.016	—	0.007	28

* In spinach chloroplasts (Fig. 3).

‡ Time at which fluorescence due to PSII (second peak in Fig. 3) is maximum.

§ Calculated from the lifetimes in the second row using the relationship $\phi = \tau/\tau_0 \cdot \tau_0$ is assumed to be 15.2 ns (2) for both photosystems.

‖ The values for PSI and PSII were obtained by directly measuring the quantum yields in digitonin fractions enriched with PSI and PSII activity.

function actinic pulse rather than one of finite width in the models. Model E allows for a larger second peak and seems to give a better fit than does Model D. This suggests that the 90 ps delay of the second kinetic peak is due to an absorbing (at 530 nm) species perhaps a carotenoid which passes energy on to PSII Chl (Model E) rather than a large difference between the vibrational relaxation time of excited Chl in PSI and PSII (Model D). Sensitized fluorescence mechanisms in photosynthesis have been observed in the past (2, 33).

Relative Fluorescent Yield of the Two Photosystems

The ratio between the lifetimes of the first and second peak in Fig. 3 is 1:20, but the ratio between the areas under the peaks (also a measure of the relative quantum yield) is 1:3. This could mean any one or all of the following: (*a*) There is more pigment associated with PSI than PSII in spinach chloroplasts as is the case in pea chloroplasts (29). This is verified using Eq. 1 in ref. 29, and the information from the last row of Table I. (*b*) Carotenoid to Chl energy transfer which is 20 to 50% efficient (34) is relatively more active in PSII (35). (*c*) PSI pigments have higher absorption coefficients at 530 nm than PSII pigments.

One might also postulate that the natural radiative lifetime of PSI Chl is less than that of PSII, but since this is not true in pea chloroplasts (27), it probably is not the case in spinach.

Energy Trapping

Several recent studies (22, 36–40) have dealt with the question of energy transfer from the absorbing accessory pigments to the trap complex. It is thought that this is accomplished by means of the intermolecular transfer of singlet electronic excitation energy probably via a mechanism involving either intermediate or weak coupling

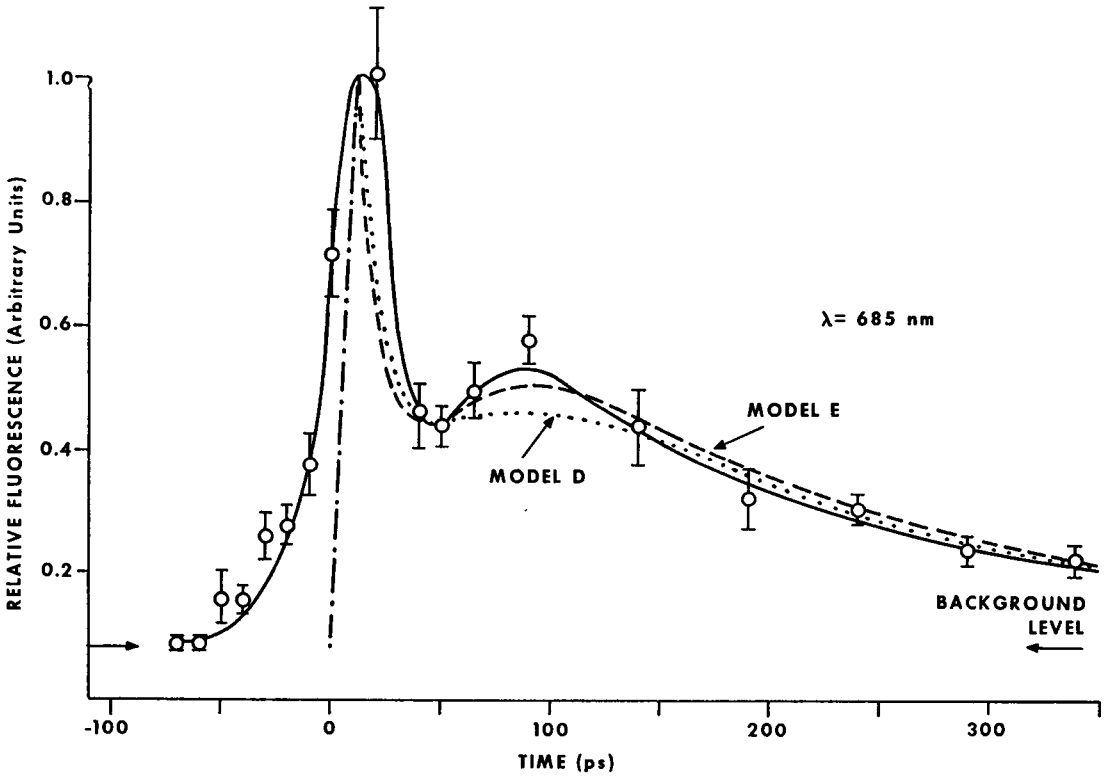

FIGURE 7 A comparison of Models D and E fitted to the data of Fig. 3. The rate constants governing the rise and fall of the first peak (see Appendix) were the same for both models ($K_1 = 0.2$ and $K_S = 0.1$). The rate constant determining the decay of the second peak, K_S' in Model D and K_S'' in Model E, was 0.005. With these values fixed, the position of the second peak (at 90 ps) is determined solely by K_1' in Model D and by K_1' and K_S' in Model E. The values used were 0.022, 0.043, and 0.042, respectively. The latter two values are not unique. The data point at 50 ps was then chosen as a reference and the height of the first peak adjusted to 1.0 by varying the ratio of $K_R\alpha_1$ and $K_R'\alpha_2$ in Model D and of $K_R\alpha_1$ and $K_R''\alpha_2K_D$ in Model E. As is seen, Model E can give a higher second peak and thus a better fit than can Model D. Rate constants are given in picoseconds^{-1}.

strength. The very short lifetimes which we observe for PSI and PSII fluorescence seem to support the former view since the expected time between successive excitation transfers which one can calculate (37–40) for both photosystems using our measurements is shorter rather than longer (37, 39) than the collisional or lattice relaxation time of Chl (~1 ps [37, 39]).

Although Chl triplet states are of little importance in the transfer of energy to PSII traps (40), their involvement in PSI photochemistry has not been eliminated. Singlet to triplet crossing times as low as 6 ps have been reported in organic dye molecules (41), triplet states of extracted Chl have been characterized by flash photolysis (42) and triplet states in vivo BChl have been observed under conditions

of low redox potential (43). Clarification of this point must await more picosecond time domain experimental evidence (19, 44).

We wish to thank Doctors D. C. DeVault, Govindjee, J. I. Krugler, D. Mauzerall, K. Sauer, and S. L. Shapiro for their encouragement and suggestions.
Messrs. P. B. Holliday, S. Hussian, and V. L. Caplan provided technical assistance.

Dr. Alfano acknowledges financial assistance from the Cottrell Research Corporation.

Received for publication 20 August 1973.

REFERENCES

1. KAMAN, M. D. 1963. Primary Processes in Photosynthesis. Academic Press, Inc., New York.
2. BRODY, S. S., and E. RABINOWITCH. 1957. *Science (Wash. D.C.)*. **125**:555.
3. DMITRIEVSKY, O., V. ERMOLAEV, and A. TERENIN. 1957. *Dokl. Akad. Nauk. S.S.S.R. (Transl.)*. **114**:468.
4. TOMITA, G., and E. RABINOWITCH. 1962. *Biophys. J.* **2**:483.
5. RUBIN, A. B., and L. K. OSNITSKAYA. 1963. *Mikrobiologiya.* **32**:200.
6. BUTLER, W. L., and K. H. NORRIS. 1963. *Biochim. Biophys. Acta.* **66**:72.
7. MURTY, N. R., and E. RABINOWITCH. 1965. *Biophys. J.* **5**:655.
8. NICHOLSON, W. J., and J. I. TORTOUL. 1967. *Biochim. Biophys. Acta.* **143**:577.
9. SINGHAL, G. S., and E. RABINOWITCH. 1969. *Biophys. J.* **9**:586.
10. MÜLLER, A., R. LUMRY, and M. S. WALKER. 1969. *Photochem. Photobiol.* **9**:113.
11. TUMERMAN, L. A., O. F. BORISOVA, AND A. B. RUBIN. 1961. *Biofizika (Transl.)*. **6**:723.
12. BRAINTAIS, J. M., H. MERKELO, and GOVINDJEE. 1972. *Photosynthetica.* **6**:133.
13. MERKELO, H., S. R. HARTMAN, T. MAR, and GOVINDJEE. 1969. *Science (Wash. D.C.)*. **164**:301.
14. YARIV, A. 1971. Introduction to Optical Electrons. Holt, Reinhart and Winston, Inc., New York.
15. MAR, T., GOVINDJEE, G. S. SINGHAL, and H. MERKELO. 1972. *Biophys. J.* **12**:797.
16. DUGUAY, M. A., and J. W. HANSEN. 1969. *Appl. Phys. Lett.* **15**:192.
17. DUGUAY, M. A. and J. W. HANSEN. 1969. *Optics Commun.* **1**:254.
18. ALFANO, R. R., and S. L. SHAPIRO. 1972. *Optics Commun.* **6**:98.
19. SEIBERT, M., R. R. ALFANO, and S. L. SHAPIRO. 1973. *Biochim. Biophys. Acta.* **292**:493.
20. SEIBERT, M., and R. R. ALFANO. 1973. *Abstr. Am. Soc. Photobiol.* MAM-C3.
21. GIORDMAINE, J. A., S. L. SHAPIRO, P. M. RENTZEPIS, and K. W. WECHT. 1967. *Appl. Phys. Lett.* **11**:216.
22. VREDENBERG, W. J., and L. N. M. DUYSENS. 1963. *Nature (Lond.)*. **197**:355.
23. SEIBERT, M., and D. DEVAULT. 1971. *Biochim. Biophys. Acta.* **253**:396.
24. AVRON, M., 1961. *Anal. Biochem.* **2**:535.
25. CRAMER, W. A., and W. L. BUTLER. 1967. *Biochim. Biophys. Acta.* **143**:332.
26. ARNON, D. I. 1949. *Plant Physiol.* **24**:1.
27. BORISOV, A. YU., and M. D. IL'INA. 1971. *Biokhimiya (Transl.)*. **36**:693.
28. BOARDMAN, N. K., S. W. THORNE, and J. M. ANDERSON. 1966. *Proc. Natl. Acad. Sci., U.S.A.* **56**: 586.
29. BORISOV, A. YU., and M. D. IL'INA. 1969. *Mol. Biol. (Transl.)*. **3**:307.
30. MOHANTY, P., B. Z. BRAUN, GOVINDJEE, and J. P. THORNBER. 1972. *Plant Cell Physiol.* **13**:81.
31. LATIMER, P., T. T. BANNISTER, and E. RABINOWITCH. 1956. *Science (Wash. D.C.)*. **124**:585.
32. MURTY, N. R., C. N. CEDERSTRAND, and E. RABINOWITCH. 1965. *Photochem. Photobiol.* **4**:917.
33. BRODY, S. S. 1957. *Rev. Sci. Instrum.* **28**:1021.
34. RABINOWITCH, E., and GOVINDJEE. 1969. *Photosynthesis.* John Wiley & Sons, Inc., New York. 158.
35. BOARDMAN, N. K. 1970. *Ann. Rev. Plant Physiol.* **21**:115.
36. BAY, Z., and R. M. PEARLSTEIN. 1963. *Proc. Natl. Acad. Sci., U.S.A.* **50**:1071.
37. CLAYTON, R. K. 1965. Molecular Physics in Photosynthesis. Blaisdell Publishing Co., New York.
38. PEARLSTEIN, R. M. 1967. *Brookhaven Symp. Biol.* **19**:8.

39. ROBINSON, G. W. 1967. *Brookhaven Symp. Biol.* **19**:16.
40. BORISOV, A. YU., and M. D. IL'INA. 1973. *Biochim. Biophys. Acta.* **305**:364.
41. RENTZEPIS, P. M., and C. J. MITSCHELE. 1970. *Anal. Chem.* **42**(14):20 *A*.
42. LIVINGSTON, R., and V. A. RYAN. 1953. *J. Am. Chem. Soc.* **75**:2176.
43. DUTTON, P. L., J. S. LEIGH, and M. SEIBERT. 1972. *Biochem. Biophys. Res. Commun.* **46**:406.
44. NETZEL, T. L., P. M. RENTZEPIS, and J. S. LEIGH. 1973. *Science (Wash. D.C.).* **182**:238.

APPENDIX

The rate equation, the solution, and the time dependence of fluorescence, $I(t)$, for each of the five models described in the Discussion and Fig. 6 are as follows:

Model A

$$dn_S'(t)/dt = K_D n_S(t) - K_S' n_S'(t) \tag{1}$$

$$n_S'(t) = \frac{K_D K_1 n_0}{K_1 - K_S}\left[\left(\frac{e^{-K_S' t} - e^{-K_S t}}{K_S - K_S'}\right) + \left(\frac{e^{-K_1 t} - e^{-K_S' t}}{K_1 - K_S'}\right)\right] \tag{2}$$

$$I(t) = K_R' n_S'(t). \tag{3}$$

In this case $K_S = K_{NR} + K_T + K_D$, $K_S' = K_R' + K_{NR}' + K_T'$, n_0 is the original number of states excited by a delta function pulse of light, $n_S(t) = (K_1 n_0/[K_1 - K_S])(e^{-K_S t} - e^{-K_1 t})$ is the number of molecules in S_1 at time t and $n_S'(t)$ is the number of molecules in S_1' at t.

Model B

$$I(t) = K_R n_S(t) + K_R' n_S'(t). \tag{4}$$

All values are the same as in Model A except that $K_S = K_R + K_{NR} + K_T + K_D$.

Model C

$$dn_S'(t)/dt = \alpha_1 K_S n_S(t) - K_S' n_S'(t) + \alpha_2 K_1' n_1'(t) \tag{5}$$

$$n_S'(t) = \frac{\alpha_1 K_D K_1 n_0}{K_1 - K_S}\left[\left(\frac{e^{-K_S' t} - e^{-K_S t}}{K_S - K_S'}\right) + \left(\frac{e^{-K_1 t} - e^{-K_S' t}}{K_1 - K_S'}\right)\right] + \frac{\alpha_2 K_1' n_0}{K_1' - K_S'}(e^{-K_S' t} - e^{-K_1' t}). \tag{6}$$

$I(t)$, K_S, K_S', and $n_S(t)$ are the same as in Model A. The constants, α_1 and α_2, are the partition fraction of photons which the two species absorb and $\alpha_2 n_1'(t)$ is the number of molecules in upper vibrational states of S_1'.

Model D

$$I(t) = \alpha_1 K_R n_S(t) + \alpha_2 K_R' n_S'(t). \tag{7}$$

The value of $n_S(t)$ is the same as in Model A, $K_S = K_R + K_{NR} + K_T$, $K_S' = K_R' + K_{NR}' + K_T'$ and $n_S'(t) = (K_1' n_0/[K_1' - K_S'])(e^{-K_S' t} - e^{-K_1' t})$.

Model E

$$I(t) = \alpha_1 K_R n_S(t) + \alpha_2 K_R'' n_S''(t). \tag{8}$$

The value of $n_S(t)$ is the same as in Model A, $K_S = K_R + K_{NR} + K_T$, $K_S' = K_{NR}' + K_T' + K_D$, $K_S'' = K_R'' + K_{NR}'' + K_T''$ and

$$n_S''(t) = \frac{K_D K_1' n_0}{K_1' - K_S'}\left[\left(\frac{e^{-K_S''t} - e^{K_S't}}{K_S' - K_S''}\right) + \left(\frac{e^{-K_1't} - e^{-K_S''t}}{K_1' - K_S''}\right)\right]$$

All the above models are subject to the boundary conditions $n_S(0) = 0$, $n_S'(0) = 0$, and $n_S''(0) = 0$.